

Three-dimensional kinematics of the tarsal joint at the trot

J. L. LANOVAZ*, S. KHUMSAP, H. M. CLAYTON, J. A. STICK† and J. BROWN†

McPhail Equine Performance Center and †Department of Large Animal Clinical Sciences, College of Veterinary Medicine, Michigan State University, East Lansing, Michigan 48824-1314, USA.

Keywords: horse; biomechanics; helical angles; attitude vector

Summary

The tarsal joint is a common site of injury for many sport horses. Understanding the biomechanics of this complex joint begins with developing a clear picture of the kinematics during normal locomotion. This study describes the 3D kinematics of the tarsal joint by measuring the motion of the tibia and third metatarsus in 4 sound Quarter Horses with targets attached directly to the bones via steel pins. The objective was to determine if the tarsus had significant motion outside the tarsocrural joint. Two Steinmann pins were inserted into the lateral side of the right hindlimb and marker triads were fixed to the end of each pin. 3D motion of the bones was recorded as each subject trotted in hand. Three rotations were expressed using an attitude vector based on the finite helical angle method. Three translations were calculated as the motion of the tibia relative to the third metatarsus. Angular and translation data were mostly coupled with flexion angle. Internal/external rotation during stance and translations during swing showed evidence of noncoupled motion. Although the majority of tarsal motion occurs in the tarsocrural joint, there is evidence that translations and rotations occur in other locations within the tarsal joint and that some of these are related to the tarsal joint 'snapping' phenomenon.

This research provides a set of reference 3D kinematics which will aid in the study of the aetiology and mechanical effects of tarsal joint lameness.

Introduction

The tarsal joint is a common site of injury for many sport horses (Gabel 1980; Winter *et al.* 1996). The majority of tarsal joint motion occurs at the tarsocrural joint and the obliquity of the trochlear surface of the talus is well known (Dyce *et al.* 1987). As a consequence, the tarsocrural joint is said to have a helical or screw action. A true helical joint has only one rotational degree of freedom and previous studies have been based on the assumption that the relevant joint motion is mainly along the sagittal plane of the horse. These kinematic studies have focused on 2D angular motion of the tarsal joint obtained from skin mounted landmarks (Kobluk *et al.* 1989; Holmström *et al.* 1994; Back *et al.* 1995; Hodson *et al.* 2001). These studies ignore any possible motion in the other two rotational degrees of freedom.

A description of true 3D motion involves not only 3 rotations, but also 3 translations. Although angular motion of the

tarsal joint has been measured in many studies, there have been a limited number of investigations into the translational motion within the joint. Schamhardt *et al.* (1984) performed an *in vitro* x-ray stereophotogrammetric study of the tarsal joint under static loading and found only submillimetre translations in any of the bones even when the limb was loaded at 1.5 times bodyweight. However, the static loading regime in that study probably does not accurately simulate physiological conditions and it does not address the action of the joint during maximum flexion, which occurs during mid-swing when the limb is unloaded.

There are good reasons as to why full 6 degree of freedom motion is not often studied with equine subjects. Artifacts are introduced into the data when the bone moves relative to the surface landmarks as the skin and underlying soft tissues slides over the bones. This noise in the kinematic data can prove especially detrimental to the calculation of 3D motion which is based on the assumption of rigid body segments (Reinschmidt *et al.* 1997). Although some correction factors have been developed to adjust for skin displacement in horses (van Weeren *et al.* 1992), these corrections are for a limited number of sites on each segment and are based on 2D analysis.

The current study addresses many of the above mentioned problems by measuring the 3D motion of the tibia and third metatarsal bones directly during normal locomotion. This was accomplished by tracking kinematic markers rigidly attached to the bones via transcutaneous intra-cortical pins. Bone pins have been used *in vivo* to study 3D kinematics in man (Lafortune *et al.* 1992) and 2D kinematics in horses (van Weeren *et al.* 1992). Degueurce *et al.* (2000) used bone pins *in vitro* to study the 3D kinematics of the metacarpophalangeal and proximal interphalangeal joints. However, the use of bone pins *in vivo* to study the 3D kinematics of equine joints has not previously been attempted.

The objective of this study was to characterise the six degree of freedom 3D motion of the equine tarsus by measuring the motion of the third metatarsus relative to the tibia during normal trotting. We aimed to test the hypothesis that the tarsal joint action is exclusively due to the screw action of the tarsocrural joint.

Materials and methods

Four sound Quarter Horses of similar weight (323, 361, 375, 416 kg) and height at the withers (144, 141, 147, 149 cm) were used in the study. The horses were judged to be free of obvious lameness during a clinical examination prior to the study. The protocol used for this investigation was approved by the University's Ethical Use Committee.

Under general anaesthesia, 4.75 mm diameter Steinmann pins were inserted into the right hindlimb. One pin was placed

*Author to whom correspondence should be addressed.

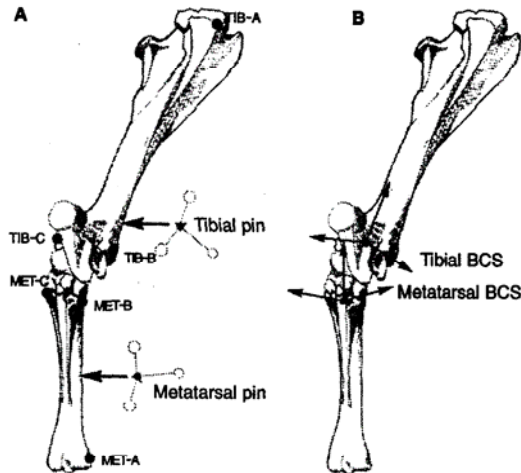


Fig 1: Locations of the palpation landmarks and bone pin insertion sites (a) and the resulting bone co-ordinate systems (BCS) for the tibia and metatarsus (b).

midlaterally in the tibia, at the level of the calcaneal tuberosity and another was placed midlaterally in the third metatarsal bone, midway along its length (Fig 1a). The pins were inserted through the lateral cortex to the edge of the medial cortex of the bone and each pin was cut off with 3 cm exposed on the lateral side of the limb. Anti-inflammatory and analgesic medication (phenylbutazone)¹ was administered before and after surgery. Data collection took place 18–20 h postsurgery and immediately after injecting local anaesthetic (mepivacane hydrochloride)² around each pin. All horses appeared pain free and moved normally during data collection.

In order to track the motion of the tibia and third metatarsus, 2 triads of kinematic markers were constructed for attachment to the Steinmann pins. Each triad consisted of 3 hollow 2.4 mm diameter stainless steel tubes arranged equidistantly around a 17 mm diameter stainless steel collar. The tubes were different lengths (6, 8 and 10 cm) and a 25 mm diameter balsa wood sphere covered with retroreflective material was attached to the end of each tube. The triad collar was designed to slide onto the Steinmann pin and the triad was secured to the pin by 2 set screws in the collar. Total mass of a triad was 38 g.

A marker triad was attached to each pin prior to the data collection session. The horses were led in hand at the trot along a 40 m rubber covered concrete runway. Three dimensional kinematic data were collected using a 6 camera analysis system³, which recorded images at a rate of 120 frames/s. The cameras were arranged in a semi-circle on one side of the runway facing the right side of the horse and a volume measuring 5 x 2 x 3 m was calibrated. For the data collection configuration used in this study, the mean error in measuring a known length was 0.88 mm. The calibrated volume was large enough to ensure the capture of more than a full stride of the right hindlimb. Data collected from a force platform⁴ embedded in the runway were synchronised with the kinematic data. Each successful trial consisted of a single stride of the right hindlimb, starting with a stance phase on the force platform. The ground reaction force data were used to detect the onset and termination of the right hind stance phase. Termination of a right hind stride was determined by an automatic algorithm that located the frame of kinematic data at

the end of the swing phase which most closely matched, in a least squares sense, the kinematic pattern at the beginning of the previous stance phase on the force plate. The kinematic data from the trot trials were filtered at 15 Hz with a fourth-order Butterworth filter. Each horse completed several strides during data collection. Four strides from each horse were selected in order to most closely match forward velocity between horses.

In order to express the kinematics of the bones in a meaningful way, coordinate systems for the tibia and third metatarsus were created based on the anatomy of the bones. Three easily palpable landmarks on each bone were chosen to define the bone based coordinate system (BCS) (Fig 1a). For the tibia, the 3 landmarks were the fibular head, at the site of attachment of the lateral collateral femoro-tibial ligament (TIB-A), the lateral malleolus (TIB-B) and the medial malleolus (TIB-C). A right-handed coordinate system was developed for the tibia by first defining the flexion/extension axis as the vector running from TIB-B to TIB-C. The adduction/abduction axis of the tibia was defined as a vector pointing cranially and perpendicular to the plane formed by the flexion/extension axis and the vector running from TIB-B to TIB-A. Finally, the internal/external rotation axis of the tibia was defined as a vector pointing proximally along the long axis of the bone perpendicular to the plane formed by the flexion/extension and adduction/abduction axes (Fig 1b). The origin of the tibial BCS was embedded in the bone midway between TIB-B and TIB-C.

For the third metatarsus BCS, the bony landmarks were located at the metatarsal attachment of the lateral collateral ligament of the metatarsophalangeal joint (MET-A), the dorsal edge of the head of the fourth metatarsal bone (MET-B), and the dorsal edge of the head of second metatarsal bone (MET-C) (Fig 1a). The third metatarsal BCS was defined in a similar manner to the tibial system. The flexion/extension axis was defined as a vector running from MET-B to MET-C. The adduction/abduction axis was defined as a vector pointing cranially and perpendicular to the plane formed by the flexion/extension axis and the vector running from MET-B to MET-A. The internal/external rotation axis was defined as pointing proximally and perpendicular to the other 2 axes, forming a right-handed coordinate system (Fig 1b). The origin of the third metatarsal BCS was embedded in the bone midway between MET-B and MET-C.

In order to develop a relationship between each BCS and the marker triads, the horse was placed in a standing position and 25 mm diameter retroreflective spheres were glued to the skin over the 3 bony landmarks that established the BCS on each bone. Kinematic data of the standing horse were collected with both the marker triads and the markers over the bony landmarks in place. Each BCS was calculated for the standing position as described above using the kinematic data from the bony landmarks. From each BCS, a transformation matrix was developed which was used to transform the locations of the triad markers in the standing position from the global kinematic coordinate system to their corresponding BCS. Since the marker triads were fixed to the bone, the relationships between the marker triad orientations and their corresponding BCS did not change. For the trotting trials, the triad markers were tracked and a singular-value decomposition method (Söderkvist and Wedin 1993) was used calculate the position and orientation of each BCS using the standing and trotting triad marker locations.

The relative angular motion between the tibia and third metatarsus was expressed in terms of a spatial attitude vector (Woltring 1994). This method is based on the finite helical axis representation of relative motion, where the position and orientation of one body with respect to another at any given

TABLE 1: The first column shows mean (s.d.) values for the 6 kinematic variables at the start of the stride for all 4 horses. The second column presents the mean of the s.d. of the start values for all horses. This gives an indication of the repeatability of the joint orientation at the start of the stride. The final column shows the mean (s.d.) ranges of motion over the stride for the variables

Kinematic variable (units)	Mean value at start of stride (s.d.)	Mean s.d. of start of stride values	Range of motion (s.d.)
Flexion(-)/extension(+) (deg)	-28.6 (1.7)	1.1	51.5 (4.1)
Adduction(+)/abduction(-) (deg)	-1.0 (2.1)	0.5	10.4 (2.0)
Internal(+)/external(-) rotation (deg)	15.8 (5.4)	0.5	6.5 (1.3)
Cranial(+)/caudal(-) translation (mm)	44.0 (9.8)	1.8	10.2 (3.0)
Medial(+)/lateral(-) translation (mm)	-8.4 (7.3)	1.5	10.4 (1.7)
Proximal(+)/distal(-) translation (mm)	89.8 (1.6)	0.9	24.3 (1.2)

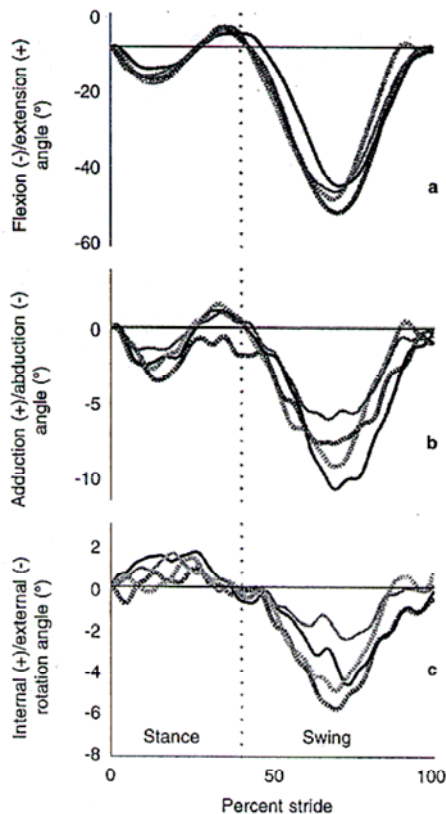


Fig 2: Angular motion curves for the tarsal joint. Each line represents an ensemble average of four strides for one subject and are referenced to their value at the start of the stride. The vertical dotted line indicates the average termination of stance.

moment can be described as a scalar rotation around, and a translation along an axis between the bodies (Woltring *et al.* 1985). The spatial attitude vector is used to describe the relative angular orientations and is calculated by multiplying the scalar finite helical angle with the components of the unit vector describing the helical axis with respect to one of the bodies. This results in 3 orthogonal angular values that are expressed in terms of the coordinate axes of one of the bodies. The angular values are independent of which body they are referenced from, only the signs are different.

In this study, following the suggestion of Woltring (1994), the spatial attitude vector was calculated with respect to the proximal segment of the joint. The angular values can be thought of as though the tibia is fixed and the third metatarsus was

moving relative to it. Therefore, the flexion(-)/extension(+), adduction(+)/abduction(-), and internal(+)/external(-) rotation components of the attitude vector that describe the angular motion of the tarsal joint are expressed in terms of the corresponding axes in the tibia.

Since there are no standard conventions for the expression of translations in the equine tarsal joint, the translation between the tibia and third metatarsus was calculated as of the motion of the origin of the tibial BCS expressed in terms of the third metatarsal BCS. Motion along the adduction/abduction axis of the metatarsus was labelled as cranial(+)/caudal(-) translation. Translation along the flexion/extension axis of the metatarsus was labelled as medial(+)/lateral(-) motion. Finally, motion along the internal/external rotation axis of the metatarsus was considered as proximal(+)/distal(-) translation. Translations were expressed as movements of the tibia relative to the third metatarsus because the metatarsal BCS is more closely aligned with the sagittal plane of the horse.

Ensemble average angle and translation curves were calculated for each horse from their 4 trials. The angular and translation data were referenced to their value at the start of the stride. To obtain a measure of the precision of the investigation, the angles and distances between the markers on each triad were calculated for every frame of each trial (Degueurce *et al.* 2000).

Results

The precision calculations resulted in overall mean standard deviation of 0.47 degrees for the angle measurements and 0.85 mm for the distance measurements. This precision is high, especially considering the size of the calibrated volume and is sufficient for the purposes of this study.

The strides used from each horse were selected to minimise velocity differences between subjects. The mean \pm s.d. velocity across all subjects was 2.83 ± 0.22 m/s, with the stance phase comprising 38.5 ± 1.6 % of the stride.

Minor conformational differences between horses were accounted for by expressing the kinematic data relative to their values at the start of the stride. This was found to be a consistent reference point. The mean s.d. of the starting values for each horse was less than 2 degrees for the angular measures and less than 2 mm for the translational measures (Table 1). Other possible reference points, such as a static standing orientation, were considered less reliable since they are difficult to replicate and the effect on the 3D tarsal joint position of assuming an arbitrary conformational orientation was not predictable.

The ranges of motion (ROM) and the impact angles for the 3 rotational motions are given in Table 1. All horses showed the same patterns of flexion/extension (Fig 2a), which included a cycle of flexion then extension during the stance phase and a larger magnitude pattern of flexion then extension during the swing phase. For the most part, the other 2 rotational degrees of

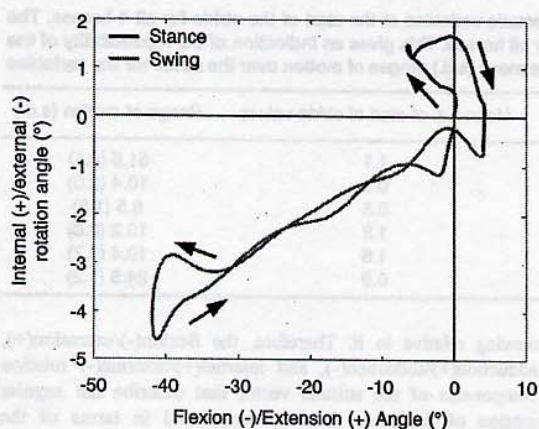


Fig 3: Typical plot of internal/external rotation angle as a function of flexion/extension angle. The stance and swing phases of the stride are indicated by the dark and light lines respectively. The data are the ensemble average of 4 strides of one horse. The arrows show the forward progression of time.

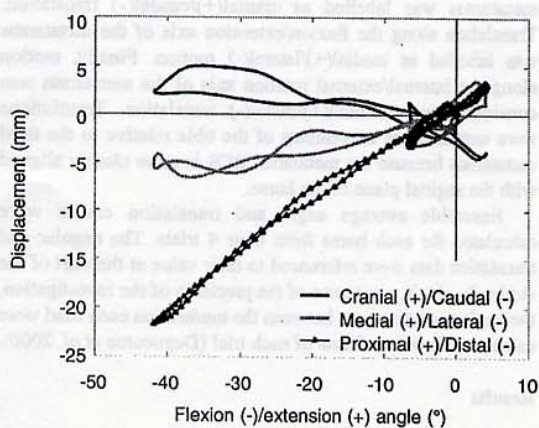


Fig 4: Typical plot of the 3 joint translations as a function of flexion/extension angle. The data are the ensemble average of 4 strides of one horse.

freedom (Fig 3) and the translational motion (Fig 4) were coupled with the flexion/extension angle, which is what should result from a screw joint motion.

The stance phase adduction/abduction angles demonstrated a small abduction motion in the first half of stance, followed in the second half of stance by a small adduction motion (Fig 2b). The swing phase showed a similar but larger pattern of abduction then adduction for all horses. For the internal/external rotation angle, all horses showed a similar movement pattern (Fig 2c), with a small internal rotation followed by a small external rotation during the stance phase. During the swing phase, all horses exhibited an external rotation followed by an internal rotation. The internal/external rotation motion during the stance phase was not well coupled with the flexion/extension angle.

The translational ROM and positions at impact are given in Table 1. All horses showed a similar pattern during the stance phase of cranial then caudal movement, lateral displacement followed by medial displacement, and distal displacement

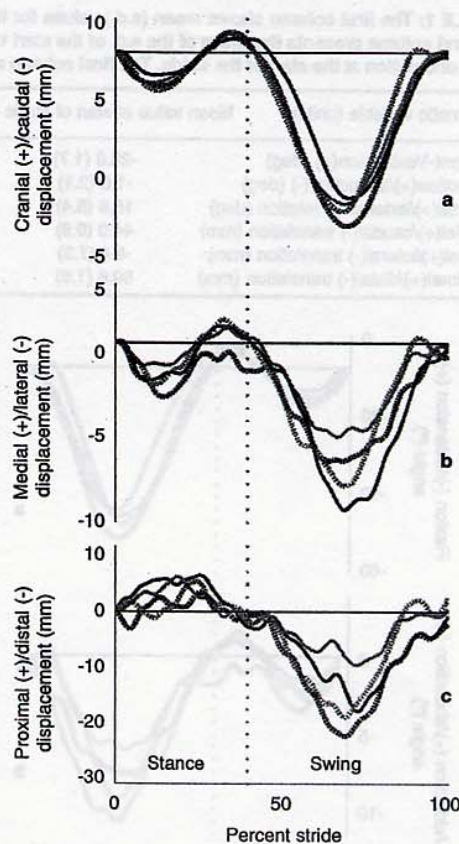


Fig 5: Translation curves for the tarsal joint. Each line represents an ensemble average of 4 strides for one subject and are referenced to their value at the start of the stride. The vertical dotted line indicates the average termination of stance.

followed by proximal displacement. These same patterns appear again, with larger magnitudes, during the swing phase (Figs 5a,b,c).

Discussion

The tarsocrural joint is assumed to dominate the motion of the tarsus, with the trochlea of the talus and the tibial cochlea acting like threads on a nut and bolt. The lack of motion observed by Schamhardt *et al.* (1984) in the smaller tarsal bones during static loading further promotes this view. Pure screw motion has a single rotational degree of freedom and a translation along the screw axis. Measurement of the screw motion of the tarsocrural joint is somewhat confounded by the fact the functional axes of the tibia and third metatarsus are not orthogonal to the screw axis of the joint. This results in additional rotational motions being measured relative to the anatomical reference frame. Since we are ultimately interested in repeatable and anatomically meaningful interpretations of the kinematic data, the use of these reference frames and the corresponding angular cross talk must be accepted.

These limitations do not prevent testing of the current study's hypothesis. In an anatomical study of the tarsal joint, Badoux (1987) found that, for the normal range of joint motion, the path that the tibia follows along the talar ridges is nearly circular, reinforcing the assumption that the tarsocrural joint has a pure screw action. Therefore, if the tarsocrural joint does behave more or less like a pure screw joint and it is the only

source of motion within the tarsal joint complex, the measured motions should all be highly coupled to the flexion/extension angle. Any noncoupled motion would be an indicator of motion outside the tarsocrural joint.

If forward velocity is taken into account, the range of motion and the shape of the flexion/extension curves in this study closely follow published trotting data calculated using 2D analysis (Kobluk *et al.* 1989; Holmström *et al.* 1994; Back *et al.* 1995), even though the flexion/extension axis of the tarsal joint defined in the current study is not necessarily perpendicular to the sagittal plane of the horse. This was expected since it has been shown that even large misalignments of the flexion/extension axis have little effect on the measured value of the flexion/extension angle for joints where flexion/extension dominates (Ramakrishnan and Kadaba 1991).

The angular motions are, for the most part, coupled, which would be expected given the screw like motion of the tarsocrural joint. There is a strong coupling between flexion/extension and adduction/abduction angles during the entire stride, with increasing abduction as flexion increases. The flexion/extension and internal/external rotation angles are also strongly coupled during most of the swing phase, showing increasing external rotation with increasing flexion (Fig 3). If the motions were perfectly coupled, values for a given internal/external rotation should be the same for a given flexion/extension angle. During mid-swing, there is a period of de-coupling which appears in varying amounts for each subject. However, during the stance phase, the internal/external rotation motion is opposite to that seen during the swing phase, showing a slight increasing internal rotation with increasing flexion. There is also a lesser degree of coupling between the rotation and flexion during the stance phase. This indicates that the joint exhibits motion during weight bearing which is not predicted by only the screw motion of tarsocrural joint.

The 3 translations are also strongly correlated to the flexion/extension angle (Fig 4). The tibial BCS origin traces a 3 dimensional circular path which generally resembles the shape of the talar trochlea. The magnitudes of the displacement are consistent with what might be predicted using the anatomical measurements of Badoux (1987). However, the translations are not completely proportional to the flexion/extension angles. The most apparent deviation is in the cranio-caudal displacement during the swing phase. At approximately 55% of the stride (25% of the swing phase), the cranial/caudal displacement 'flattens' out and becomes asymmetric with respect to the swing phase flexion peak. This produces hysteresis when the translations are plotted with respect to the flexion/extension angle i.e. the translation follows a different path during flexion and extension (Fig 4). One explanation for this behaviour is the superposition of some caudal motion of the tibia/talus with respect to the third metatarsus outside of the tarsocrural joint during mid swing. There is evidence of similar caudal translations, although to a smaller degree, in the stance phase, as well as some medial translation during mid stance and mid swing. Since this study measures only the motion of the tibia relative to the third metatarsus, it was not possible to determine the amount and type of motion occurring at the individual joints within the tarsal joint complex. However, given the assumption of circular talar ridges (Badoux 1987), even conservative estimations indicate movement at the other tarsal joints many times larger than what has been previously reported (Schamhardt *et al.* 1984).

A phenomenon of the tarsal joint that has often been reported is the 'clicking' or 'snapping' motion (Updike 1984; Badoux 1987; Alexander and Trestik 1989; Back *et al.* 1995) that occurs in early and late swing. It has been shown that the collateral ligaments (CL) play a crucial role in this action (Updike 1984;

Alexander and Trestik 1989). The snapping action is described as the joint moving rapidly into maximal flexion or extension as the joint passes through a critical mid-point angle (Alexander and Trestik 1989). The snapping action is thought to come from the fact that the CL have eccentric attachments relative to the centre of rotation of the tarsocrural joint (Updike 1984; Badoux 1987; Alexander and Trestik 1989). Evidence of the snapping motion may be visible in this study. The cranio-caudal translation becomes de-coupled with the flexion/extension motion in early swing at about -50 degrees of flexion and becomes coupled again later in swing as the joint passes back through that point of flexion. This angle corresponds almost exactly with the angle at which the snapping motion occurs as reported by Badoux (1987) and Alexander and Trestik (1989) and very near the inflection point in the flexion profile reported by Back *et al.* (1995) that is also suspected of being associated with the snapping action. Alexander and Trestik (1989) proposed a bistable model of the joint where the snapping motion is related to the tension in and position of the CL and used a 2D analysis to relate the action to a single rotational degree of freedom in the tarsocrural joint. The current study shows that perhaps there is also an effect on the motion at other joints of the tarsal complex and that it may affect motion in other directions.

In conclusion, this study presents full 3D kinematics describing the relative motion of the tibia and third metatarsus, which are the long bones proximal and distal to the tarsal joint complex. We tested the hypothesis that the motion of the tarsal joint is exclusively due to the screw action of the tarsocrural joint and found that the results did not support this hypothesis. The majority of the tarsal joint motion can be attributed to the tarsocrural joint, but there is evidence that some measurable translations and rotations, both in swing and stance, occur in other locations within the tarsal joint complex. There are also indications that some of these motions are related to the ligamentous 'snapping' phenomenon that occurs during early and late swing.

Acknowledgements

This study was supported by the Mary Anne McPhail Endowment, Michigan State University. The authors would like to thank Carissa Wickens and Sarah Fox for assistance during data collection.

Manufacturers' addresses

¹Schering-Plough Animal Health Corp., Union, New Jersey, USA.

²Pharmacia & Upjohn Company, Kalamazoo, Michigan, USA.

³Motion Analysis Corporation, Santa Rosa, California, USA.

⁴Advanced Mechanical Technology, Inc., Watertown, Massachusetts, USA.

References

- Alexander, R.McN. and Trestik, C.L. (1989) Bistable properties of the hock joint of horses (*Equus spp.*). *J. Zool.* **218**, 383-391.
- Back, W., Schamhardt, H.C., Savelberg, H.H.C.M., Bogert, A.J. van den, Bruin, G., Hartman, W. and Barneveld, A. (1995) How the horse moves: 2. Significance of graphical representations of equine hind limb kinematics. *Equine vet. J.* **27**, 39-45.
- Badoux, D.M. (1987) Some biomechanical aspects of the structure of the equine tarsus. *Anat. Anz.* **164**, 53-61.
- Degueurce, C., Chateau, H., Pasqui-Boutard, V., Pourcelot, P., Audigé, F., Crevier-Denoix, N., Jerbi, H., Geiger, D. and Denoix, J.-M. (2000) Concrete use of the joint coordinate system for the quantification of articular rotations in the digital joints of the horse. *Vet. Res.* **31**, 297-311.
- Dyce, K.M., Sack, W.O. and Wensing, C.J.G. (1987) The skeleton of the leg and hock; The hock joint. In: *Textbook of Veterinary Anatomy*, W.B. Saunders Company, Philadelphia. pp 582-584

- Gabel, A.A. (1980) Lameness caused by inflammation in the distal hock. *Vet. Clin. N. Am.: Large Anim. Pract.* 2, 101-124.
- Hodson, E.F., Clayton, H.M. and Lanovaz, J.L. (2001) The hind limb in walking horses: 1. Kinematics and ground reaction forces. *Equine vet. J.* 33, 38-43.
- Holmström, M., Fredricson, I. and Drevemo, S. (1994) Biokinematic analysis of the Swedish Warmblood riding horse at trot. *Equine vet. J.* 26, 235-240.
- Kobluk, C.N., Schnurr, D., Horney, F.D., Hearn, T.C., Summer-Smith, G., Willoughby, R.A. and DeKleer, V.S. (1989) Use of high speed cinematography and computer generated gait diagrams for the study of equine hind limb kinematics. *Equine vet. J.* 21, 48-58.
- Lafortune, M.A., Cavanagh, P.R., Sommer III, H.J. and Kalenak, A. (1992) Three-dimensional kinematics of the human knee during walking. *J. Biomech.* 25, 347-357.
- Ramakrishnan, H.K. and Kadaba, M.P. (1991) On the estimation of joint kinematics during gait. *J. Biomech.* 24, 969-97.
- Reinschmidt, C., Bogert, A.J. van den, Nigg, B.M., Lundberg, A. and Murphy, N. (1997) Effect of skin movement on the analysis of skeletal knee joint motion during running. *J. Biomech.* 30, 729-732.
- Schamhardt, H.C., Hartman, W. and De Lange, A. (1984) Kinematics of the equine tarsus. *XV Congress of the European Association of Veterinary Anatomists. Abstracts.* pp 178-179.
- Söderkvist, I. and Wedin, P. (1993) Determining the movements of the skeleton using well-configured markers. *J. Biomech.* 26, 1473-1477.
- Updike, S.J. (1984) Functional anatomy of the equine tarsocrural collateral ligaments. *Am. J. vet. Res.* 45, 867-874.
- Weeren, P.R. van, Bogert, A.J. van den and Barneveld, A. (1992) Correction models for skin displacement in equine kinematic gait analysis. *J. equine vet. Sci.* 12, 178-192.
- Winter, D., Bruns, E., Glodek, P. and Hertsch, B. (1996) Genetic disposition of bone diseases in sport horses. *Zuchungskunde* 68, 92-108.
- Woltring, H.J. (1994) 3D attitude representation of human joints: a standardisation proposal. *J. Biomech.* 27, 1399-1414.
- Woltring, H.J., Huiskes, R., De Lange, A. and Veldpaus, F. (1985) Finite centroid and helical axis estimation from noisy landmark measurements in the study of human joint kinematics. *J. Biomech.* 18, 379-389.